IL NUOVO CIMENTO Vol. 35 C, N. 6 Novembre-Dicembre 2012
DOI 10.1393/ncc/i2012-11385-3

Colloquia: LaThuile12

# Search for the Standard Model Higgs boson at ATLAS

J. Tanaka on behalf of the ATLAS Collaboration

*International Center for Elementary Particle Physics and Department of Physics*
*The University of Tokyo - Tokyo, Japan*

ricevuto il 7 Settembre 2012

**Summary.** — A search for the Standard Model Higgs boson has been performed with the ATLAS experiment at the LHC using data corresponding to integrated luminosities from $1.04\,\text{fb}^{-1}$ to $4.9\,\text{fb}^{-1}$ of $pp$ collisions collected at $\sqrt{s} = 7\,\text{TeV}$ in 2011. The Higgs boson mass ranges 112.9–115.5 GeV, 131–238 GeV and 251–466 GeV are excluded at the 95% confidence level, while the range 124–519 GeV is expected to be excluded in the absence of a signal. An excess of events is observed around the mass of 126 GeV with a local significance of 3.5 standard deviations. The global probability for the background to produce such a fluctuation anywhere in the explored Higgs boson mass range 110–600 GeV is estimated to be $\sim 1.4\%$, or 2.2 standard deviations from the background-only hypothesis.

PACS 14.80.Bn – Standard-model Higgs bosons.

## 1. – Introduction

The discovery of the Standard Model (SM) Higgs boson [1-3] is one of the primary goals of the ATLAS experiment [4] at the Large Hadron Collider (LHC) [5], to understand the mechanism of electroweak symmetry breaking and the origin of mass of elementary particles. Direct searches at the CERN LEP $e^+e^-$ collider excluded the production of a SM Higgs boson with mass below 114.4 GeV at the 95% confidence level (CL) [6]. Searches at the Fermilab Tevatron $p\bar{p}$ collider have excluded the production of a Higgs boson with mass between 156 GeV and 177 GeV at the 95% CL [7].

In 2011, the ATLAS experiment collected and analysed data with an integrated luminosity up to $4.9\,\text{fb}^{-1}$ fulfilling all the data quality requirements to search for the SM Higgs boson. In this paper, the analysis and results of three different channels, $H \to \gamma\gamma$ [8], $H \to ZZ^{(*)} \to \ell^+\ell^-\ell'^+\ell'^-$ [9], and $H \to WW^{(*)} \to \ell^+\nu\ell'^-\bar{\nu}$ [10] are briefly summarized. A combined search [11] is presented which includes also $H \to ZZ \to \ell^+\ell^-\nu\bar{\nu}$ [12], $H \to ZZ \to \ell^+\ell^-q\bar{q}$ [13] and $H \to WW \to \ell\nu q\bar{q}'$ [14] channels, covering a mass range of 110–600 GeV.

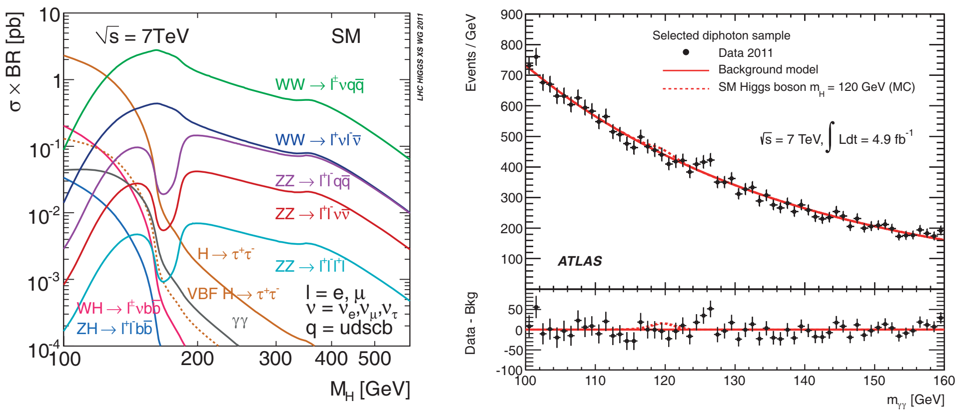


Fig. 1. – Left: SM Higgs boson production cross section times branching ratio [15] for several SM Higgs boson decay channels as a function of Higgs boson mass. Right: Invariant-mass distribution [8] for the inclusive data sample, overlaid with the sum of the background-only fits in different categories and the signal expectation for a mass hypothesis of 120 GeV corresponding the the SM cross section. The figure below displays the residual of the data with respect to the background-only fit sum.

## 2. – Analysis and results of specific channels

The products of production cross sections and decay branching ratios for several SM Higgs channels are shown in fig. 1 (left). $H \to \gamma\gamma$ is important in a low Higgs mass range ($m_H < 150\,\text{GeV}$). Five other channels contribute to the entire mass range considered. However due to the difficulty of suppressing the the main backgrounds, only $H \to ZZ^{(*)} \to \ell^+\ell^-\ell'^+\ell'^-$ and $H \to WW^{(*)} \to \ell^+\nu\ell'^-\bar{\nu}$ are analysed down to a Higgs mass of 110 GeV.

**2**·1. $H \to \gamma\gamma$ *channel*. – The search for $H \to \gamma\gamma$ [8] is performed for Higgs boson masses between 110 and 150 GeV using $4.9\,\text{fb}^{-1}$. The event selection requires two isolated, high transverse momentum ($p_T$) photons with $p_T > 40\,\text{GeV}$ and 25 GeV. Selected events are separated into nine independent categories. This categorisation is based on the direction of each photon and whether it was reconstructed as a converted or unconverted photon, together with the momentum component of the diphoton system transverse to the thrust axis defined by the diphoton system. The diphoton invariant mass $m_{\gamma\gamma}$ is used as a discriminating variable to separate signal from background, to take advantage of the good mass resolution of approximately 1.4% for $m_H \sim 120\,\text{GeV}$. The distribution of $m_{\gamma\gamma}$ in the data is fitted to an exponential function to estimate the background. The inclusive invariant mass distribution of the observed candidates, summing over all the categories, is shown in fig. 1 (right).

The observed and expected local $p_0$ values and 95% CL upper limits on the Higgs boson production cross section divided by the SM prediction are shown in fig. 2. (The statistical methods used are described in sect. **3**.) The largest excess with respect to the background-only hypothesis in the mass range of 110–150 GeV is observed at 126.5 GeV with a local significance of 2.9 standard deviations. When the uncertainties on photon energy scale and also the look-elsewhere effect in the mass range of 110–150 GeV are taken into account, this excess becomes 1.5 standard deviations. The median expected

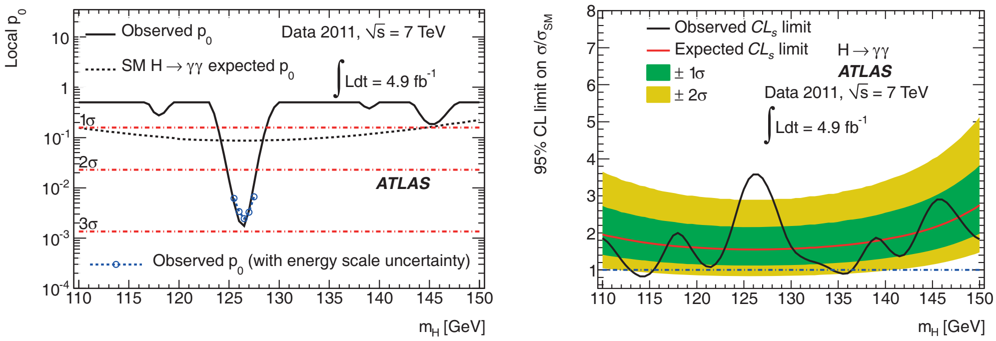


Fig. 2. – Left: The expected and observed local $p_0$ [8]. The open points indicate the observed local $p_0$ value when energy scale uncertainties are taken into account. Right: The expected and observed 95% CL upper limits [8] on the SM Higgs boson production normalized to the predicted cross section as a function of $m_H$.

upper limits of the cross section at the 95% CL vary between 1.6 and 2.7 in the mass range of 110–150 GeV while the observed limit varies between 0.83 and 3.6. A SM Higgs boson is excluded at the 95% CL in the mass ranges of 113–115 GeV and 134.5–136 GeV.

**2**·2. *$H \to ZZ^{(*)} \to \ell^+\ell^-\ell'^+\ell'^-$ channel.* – The search for $H \to ZZ^{(*)} \to \ell^+\ell^-\ell'^+\ell'^-$ [9] is carried out for Higgs boson masses between 110 GeV and 600 GeV using 4.8 fb$^{-1}$. Three different categories based on lepton flavor are introduced; $e^+e^-e^+e^-$, $e^+e^-\mu^+\mu^-$ and $\mu^+\mu^-\mu^+\mu^-$. Higgs boson candidates are selected by requiring two same-flavour, opposite-sign isolated lepton pairs in an event. These four leptons are required to have $p_T > 20$, 20, 7 and 7 GeV. The invariant mass of the lepton pair closest to $Z$ boson mass is required to be within 15 GeV of the known $Z$ mass, while that of another lepton pair is required to be smaller than 115 GeV and larger than 15–60 GeV depending on the four-lepton invariant mass ($m_{4\ell}$). The dominant irreducible $ZZ^{(*)}$ background is estimated using Monte Carlo simulation. The reducible $Z$+jets background, which becomes important in the low mass range, is estimated from control regions in the data. The top-quark background normalisation is validated in a control sample. The mass resolutions are approximately 1.5% in the four-muon channel and 2% in the four-electron channel for $m_H \sim 130$ GeV. The four-lepton invariant mass is used as a discriminating variable as shown in fig. 3 (left) for the low mass range and fig. 3 (right) for the full mass range.

Figure 4 (left) shows the observed and expected 95% CL cross section upper limits as a function of $m_H$. A SM Higgs boson is excluded at 95% CL in the mass ranges 134–156 GeV, 182–233 GeV, 256–265 GeV and 268–415 GeV. The expected exclusion ranges are 136–157 GeV and 184–400 GeV. Figure 4 (right) shows the local $p_0$ as a function of $m_H$. The most significant upward deviations from the background-only hypothesis are observed for $m_H = 125$ GeV with a local $p_0$ of 1.6% (2.1$\sigma$), $m_H = 244$ GV with a local $p_0$ of 1.3% (2.2$\sigma$), and $m_H = 500$ GV with a local $p_0$ of 1.8% (2.1$\sigma$). When the look-elsewhere effect is taken into account, the global $p_0$ for each excess becomes $O(50\%)$.

**2**·3. *$H \to WW^{(*)} \to \ell^+\nu\ell'^-\bar{\nu}$ channel.* – The search for $H \to WW^{(*)} \to \ell^+\nu\ell'^-\bar{\nu}$ [10] is performed as an event counting analysis for Higgs boson masses between 110 GeV and

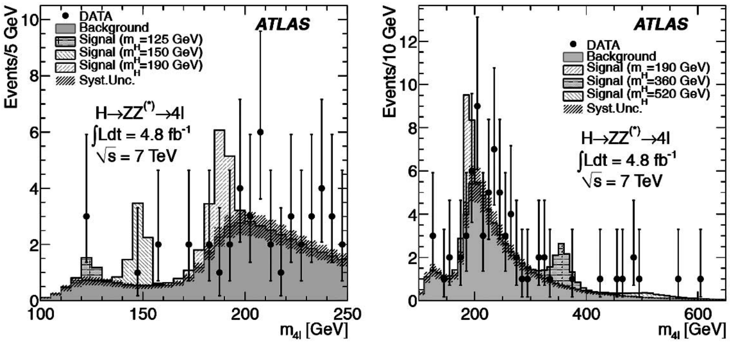


Fig. 3. – $m_{4\ell}$ distribution [9] of the selected candidates, compared to the background expectation for the 100–250 GeV mass range (left) and the full mass range of the analysis (right). The signal expectation for several $m_H$ hypothesis is also shown.

300 GeV using 2.05 fb$^{-1}$. Events are required to have two opposite-sign isolated leptons with $p_T > 20$ GeV for electron and 15 GeV for muon. The leading lepton $p_T$ must be larger than 25 GeV to match a trigger requirement. Because of the presence of two neutrinos from $W$ boson decay, a large missing transverse momentum ($E_{\mathrm{T}}^{\mathrm{miss}}$) is required. Figure 5 (left) shows the distribution of the quantity $E_{\mathrm{T,rel}}^{\mathrm{miss}}$, which is defined as $E_{\mathrm{T}}^{\mathrm{miss}}$ if the angle $\Delta\phi$ between the missing transverse mass and the transverse momentum of the nearest lepton or jet is greater than $\pi/2$, or $E_{\mathrm{T}}^{\mathrm{miss}} \sin(\Delta\phi)$ otherwise. Good agreement between real data and Monte Carlo simulation is observed. In addition, since the direction of two leptons from $W$ boson decay are preferentially close, due to the spin quantum numbers of Higgs and $W$ bosons, a small angle between the two leptons, as well as a low invariant mass of two leptons ($m_{\ell\ell^{(\prime)}}$) are required. The selected events are separated into 0-jet and 1-jet categories as well as according to lepton flavour. Figure 5 (right) shows the jets multiplicity distribution. Non-resonant $WW$ is dominant in the 0-jet category, and top-quark production is dominant in the 1-jet category. The non-resonant $WW$ production is estimated from the data using control regions based on $m_{\ell\ell^{(\prime)}}$. In the

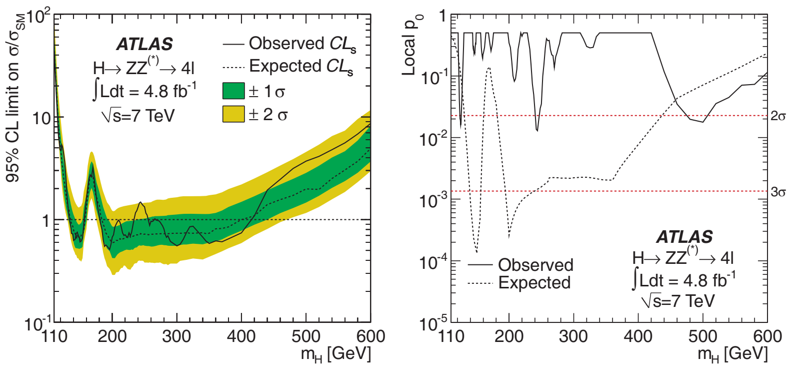


Fig. 4. – The expected and observed 95% CL upper limits (left) [9] and local $p_0$ (right) [9] as a function of $m_H$.

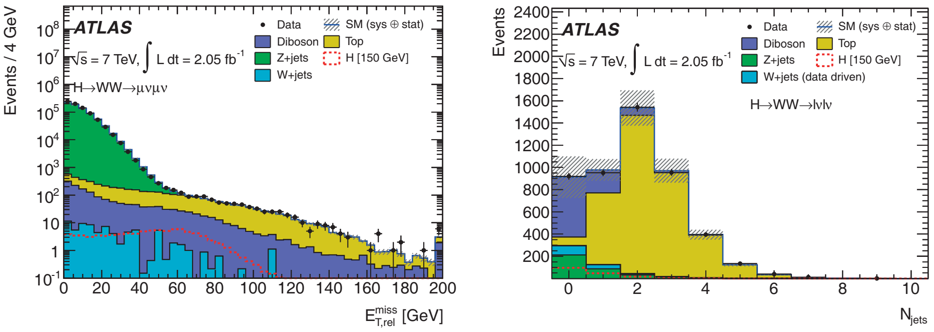


Fig. 5. – Left: The $E_{\mathrm{T,rel}}^{\mathrm{miss}}$ distribution [16] of the $H \to WW^{(*)} \to \mu^+\nu\mu'^-\bar{\nu}$ channel after the requirement of lepton $p_T$ and $m_{\ell\ell}$. Right: Multiplicity of jets [16] with $p_T > 25\,\mathrm{GeV}$ after the cut on $E_{\mathrm{T,rel}}^{\mathrm{miss}}$.

1-jet category, a $b$-jet veto is applied to reject events from top-quark production. The transverse mass distribution of events for both jet categories is shown in fig. 6.

Figure 7 (left) shows the expected and observed limits. The mass range of 145–206 GeV is excluded at 95% CL while the median expected limit excludes the mass range of 134–200 GeV. Figure 7 (right) shows the local $p_0$ and no significance deviation from background is observed.

## 3. – Combination

Figure 8 show results from six different channels, which are combined [11] by using the profile likelihood ratio. The signal strength, $\mu$, is defined as $\mu = \sigma/\sigma_{\mathrm{SM}}$, where $\sigma$ is the Higgs boson production cross section being tested and $\sigma_{\mathrm{SM}}$ its SM value. The signal strength is extracted from the full likelihood including all the parameters describing the systematic uncertainties and their correlations. The details of this procedure are found in refs. [17, 18]. Exclusion limits are based on the $CL_S$ method [19] and a value of $\mu$ is regarded as excluded at the 95% CL when $CL_S$ takes on the corresponding value.

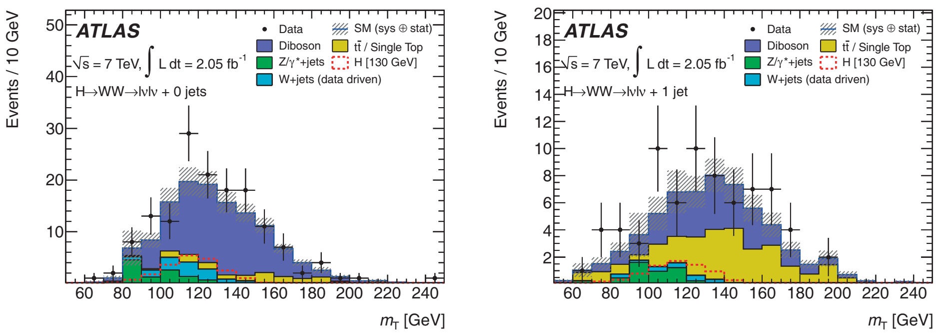


Fig. 6. – The transverse mass distribution [16] of events for the 0-jet (left) and 1-jet (right) categories. The expected signal is also shown for $m_H = 130\,\mathrm{GeV}$.

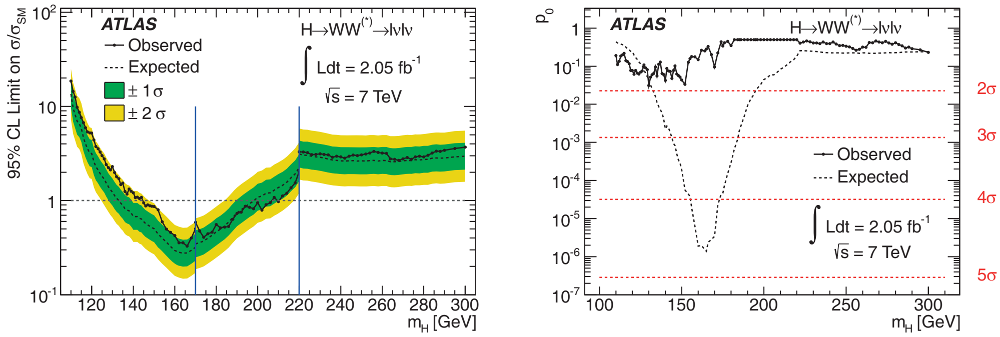


Fig. 7. – The expected and observed 95% CL upper limits (left) [10] and local $p_0$ (right) [16] as a function of $m_H$.

The combined 95% CL exclusion limits on $\mu$ are shown in fig. 9 (left) for the full mass range and fig. 9 (right) for the low mass range. These results are based on the asymptotic approximation described in [20]. The Higgs boson mass ranges 112.9–115.5 GeV, 131–238 GeV and 251–466 GeV are excluded at the 95% CL, while the range 124–519 GeV is expected to be excluded in the absence of a signal.

In fig. 9 (right), an excess of events is observed at $m_H \sim 126$ GeV. Such an excess can be tested by the probability ($p_0$) that a background-only experiment fluctuates to be more signal-like than what is observed. The equivalent formulation in terms of number of standard deviations is referred to as the significance. The profile likelihood ratio test statistic is defined such that $p_0$ cannot exceed 50%. The local $p_0$ probability and significance are defined for a fixed $m_H$ hypothesis and then the global $p_0$ probability and significance are evaluated by taking the look-elsewhere effect [17, 21] into account. Figure 10 (left) shows the local $p_0$ as a function of $m_H$. The largest local significance in the combination is found at $m_H = 126$ GeV, where it reaches $3.6\sigma$ with an expected value of $2.5\sigma$ for a SM Higgs boson signal. The observed (expected) local significance for $m_H = 126$ GeV is $2.8\sigma$ ($1.4\sigma$) in the $H \to \gamma\gamma$ channel, $2.1\sigma$ ($1.4\sigma$) in the $H \to ZZ^{(*)} \to \ell^+\ell^-\ell'^+\ell'^-$ channel, and $1.4\sigma$ ($1.4\sigma$) in the $H \to WW^{(*)} \to \ell^+\nu\ell'^-\bar{\nu}$ channel. By taking

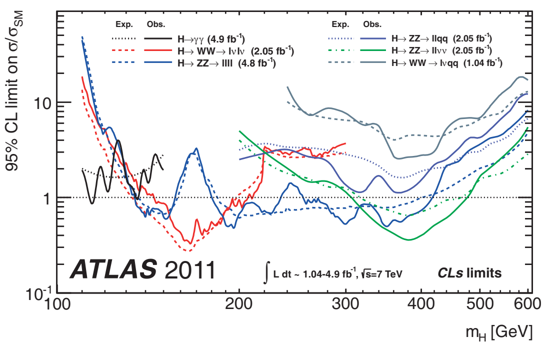


Fig. 8. – The expected and observed cross section limits for the individual search channels [22].

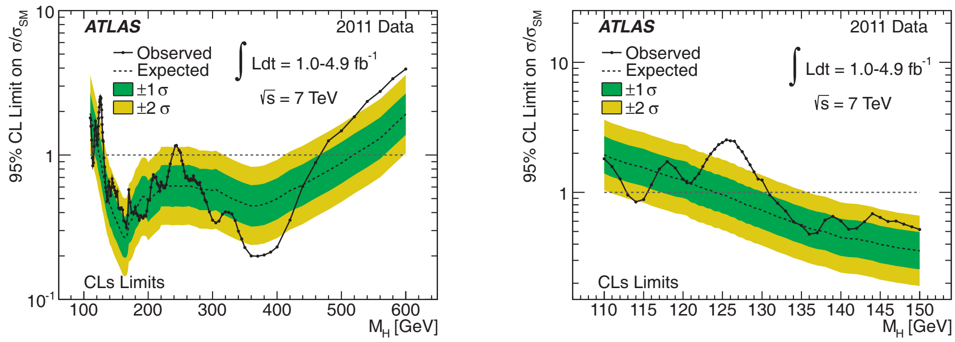


Fig. 9. – The expected and observed 95% CL upper limits [22] on the SM Higgs boson production normalized to the predicted cross section for the full (left) and the low-mass (right) range.

into account the systematic uncertainties on energy scale, this excess slightly reduces from $3.6\sigma$ to $3.5\sigma$. The global $p_0$ for this combined $3.5\sigma$ excess to be found anywhere in the mass range 110–600 GeV is 1.4% ($2.2\sigma$).

Figure 10 (right) shows the best-fit signal strength $\mu$ as a function of $m_H$ for the low-mass range. The $\mu$ value indicates by what factor the SM Higgs boson cross section would have to be scaled to match to the observed data and the excess observed at $m_H = 126\,\text{GeV}$ corresponds to a value of $\mu$ of approximately $1.5^{+0.5}_{-0.6}$, which is consistent with the signal expected from a SM Higgs boson at that mass.

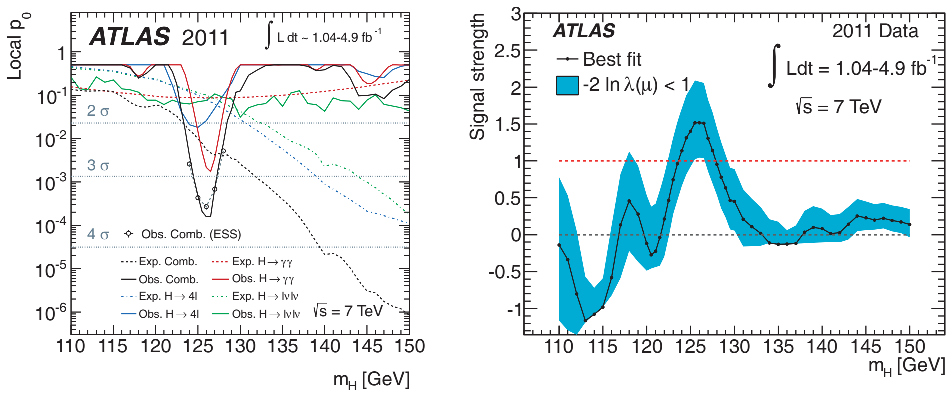


Fig. 10. – Left: The expected and observed local $p_0$ as a function of $m_H$ [11]. The solid curves give the individual and combined observed $p_0$, estimated using the asymptotic approximation. The dashed curves show the median expected value for the hypothesis of a SM Higgs boson signal at that mass. The points indicate the observed local $p_0$ estimated using ensemble tests and taking into account energy scale systematic uncertainties. Right: The best-fit signal strength $\mu$ as a function of $m_H$ for the low mass range [22].

## 4. – Conclusion

A search for the Standard Model Higgs boson has been performed with the ATLAS experiment at the LHC using data corresponding to integrated luminosities from $1.04\,\mathrm{fb}^{-1}$ to $4.9\,\mathrm{fb}^{-1}$ of *pp* collisions collected at $\sqrt{s} = 7\,\mathrm{TeV}$ in 2011. The Higgs boson mass ranges 112.9–115.5 GeV, 131–238 GeV and 251–466 GeV are excluded at the 95% CL, while the range 124–519 GeV is expected to be excluded in the absence of a signal. An excess of events is observed around the mass of 126 GeV with a local significance of $3.5\sigma$. The local significance of $H \to \gamma\gamma$, $H \to ZZ^{(*)} \to \ell^+\ell^-\ell'^+\ell'^-$, $H \to WW^{(*)} \to \ell^+\nu\ell'^-\bar{\nu}$, the three most sensitive channels in this mass range, are $2.8\sigma$, $2.1\sigma$ and $1.4\sigma$, respectively. The global probability for the background to produce such a fluctuation anywhere in the explored Higgs boson mass range 110–600 GeV is estimated to be $\sim 1.4\%$.

Finally, an integrated luminosity of $15\,\mathrm{fb}^{-1}$ is expected at $\sqrt{s} = 8\,\mathrm{TeV}$ in 2012. With this data, it might be possible either to discover the SM Higgs boson of mass around 120–131 GeV or to exclude the mass range of 115.5–131 GeV.

REFERENCES


[1] Englert F. and Brout R., *Phys. Rev. Lett.*, **13** (1964) 321.
[2] Higgs P., *Phys. Rev. Lett.*, **12** (1964) 132; **13** (1964) 508.
[3] Guralnik G. S., Hagen C. R. and Kibble T. W. B., *Phys. Rev. Lett.*, **13** (1964) 585.
[4] ATLAS Collaboration, *JINST*, **3** (2008) S08003.
[5] Evans L. and Bryant P., *JINST*, **3** (2008) S08001.
[6] ALEPH, DELPHI, L3 and OPAL Collaborations and the LEP Working Group for Higgs boson searches, *Phys. Lett. B*, **565** (2003) 61.
[7] TEVNPH (Tevatron New Phenomena and Higgs Working Group), arXiv:1107:5518.
[8] ATLAS Collaboration, *Phys. Rev. Lett.*, **108** (2012) 111803.
[9] ATLAS Collaboration, *Phys. Lett. B*, **710** (2012) 383.
[10] ATLAS Collaboration, *Phys. Rev. Lett.*, **108** (2012) 111802.
[11] ATLAS Collaboration, *Phys. Lett. B*, **710** (2012) 49.
[12] ATLAS Collaboration, ATLAS-CONF-2011-148 (https://cdsweb.cern.ch/record/1392668).
[13] ATLAS Collaboration, *Phys. Lett. B*, **707** (2012) 27.
[14] ATLAS Collaboration, *Phys. Rev. Lett.*, **107** (2011) 231801.
[15] LHC Higgs Cross Section Working Group, CERN-2011-002, arXiv:1101:0593.
[16] ATLAS Collaboration, https://atlas.web.cern.ch/Atlas/GROUPS/PHYSICS/PAPERS/HIGG-2011-08/.
[17] ATLAS and CMS Collaborations, LHC Higgs Combination Working Group Report, ATL-PHYS-PUB-2011-011 (https://cdsweb.cern.ch/record/1375842) CMS-NOTE-2011-005 (https://cdsweb.cern.ch/record/1379837).
[18] ATLAS Collaboration, *Eur. Phys. J. C*, **71** (2010) 1782.
[19] Read A. L., *J. Phys. G*, **28** (2002) 2693.
[20] Cowan G., Crammer K., Gross E. and Vitells O., *Eur. Phys. J. C*, **71** (2010) 1554.
[21] Gross E. and Vitells O., *Eur. Phys. J. C*, **70** (2010) 525.
[22] ATLAS Collaboration, https://atlas.web.cern.ch/Atlas/GROUPS/PHYSICS/PAPERS/HIGG-2012-03/.